ETH
Eidgenössische Technische Hochschule Zürich
Swiss Federal Institute of Technology Zurich

Seminar for Applied Mathematics SAM

Schemes with Well controlled Dissipation (WCD) I: Non-classical shock waves

J. Ernest and P. LeFloch and S. Mishra

Research Report No. 2013-41
November 2013

Seminar für Angewandte Mathematik
Eidgenössische Technische Hochschule
CH-8092 Zürich
Switzerland

Funding ERC: 306279 SPARCCLE

SCHEMES WITH WELL-CONTROLED DISSIPATION (WCD). NONCLASSICAL SHOCK WAVES

JAN ERNEST[1], PHILIPPE G. LEFLOCH[2], AND SIDDHARTHA MISHRA[1]

Abstract. We consider the approximation of entropy solutions to nonlinear hyperbolic conservation laws, in the regime that small–scale effects drive the dynamics of shock waves in these solutions. We introduce and analyze a new class of numerical methods, referred to as the schemes with *well-controled dissipation (WCD),* which approximate entropy solutions with high–accuracy and can capture small scale dependent shock waves of arbitrary strength. Following earlier work by LeFloch and collaborators, we rely on the equivalent equation associated with a finite difference scheme which provides us with the proper tool in order to ensure that small-scale dependent shock waves are computed accurately. Examples involving nonclassical shocks for cubic conservation laws, the nonlinear elasticity system, and a reduced model of magnetohydrodynamics are investigated with our approach.

1. Introduction.

1.1. Hyperbolic systems of conservation laws. Many interesting phenomena in physics and engineering are modeled by systems of nonlinear hyperbolic partial differential equations (PDE's) which often take the form of systems of conservation laws:

$$\mathbf{U}_t + \mathbf{F}(\mathbf{U})_x = 0. \tag{1.1}$$

Here, $\mathbf{U} = \mathbf{U}(t,x)$ is a vector-valued unknown, while the map $\mathbf{F} = \mathbf{F}(\mathbf{U})$ is a prescribed flux vector. This system (1.1) must be supplemented with initial and boundary conditions, and it is well-known that solutions can contain discontinuities such as shock waves and contact discontinuities, even when the initial data is smooth [12, 22]. Hence, the solutions to systems of conservation laws are interpreted in the sense of distributions. These *weak* solutions need not be unique, and admissibility criteria are needed in order to single out physically relevant solutions. These admissibility criteria are termed *entropy conditions*. More specifically, physically relevant solutions to (1.1) should satisfy the *entropy inequality*

$$S(\mathbf{U})_t + Q(\mathbf{U})_x \leq 0. \tag{1.2}$$

Here, the entropy function S and the associated entropy flux Q are related by $DQ = DS \cdot D\mathbf{F}$.

1.2. Small-scale dependent shock waves. It is also well-known that several small-scale effects such as diffusion, dispersion, capillarity, Hall effect, etc have been neglected in the course of the derivation of the system of conservation laws (1.1) in any given physical context. Keeping such small-scale terms often (but not always) results in "regularized" diffusive-dispersive systems of conservation laws of the form [27, Chap. 1]:

$$\mathbf{U}_t + \mathbf{F}(\mathbf{U})_x = \epsilon\big(B(\mathbf{U})\mathbf{U}_x\big)_x + \alpha\epsilon^2\big(C_1(\mathbf{U})(C_2(\mathbf{U})\mathbf{U}_x)_x\big)_x. \tag{1.3}$$

[1]Seminar for Applied Mathematics (SAM) & D-Math, ETH, HG Raemistrasse, Zürich-8092, Switzerland. Email: jernest@bluewin.ch, smishra@sam.math.ethz.ch.

[2] Laboratoire Jacques-Louis Lions & Centre National de la Recherche Scientifique, Université Pierre et Marie Curie (Paris 6), 75258 Paris, France. Email: contact@philippelefloch.org

[0]SM was partially supported by the ERC starting grant 306279: SPARCCLE

Here, the matrix-valued field $B = B(\mathbf{U})$ models diffusive effects whereas the dispersive effects (capillarity, Hall effect etc) are modeled by the maps $C_1 = C_1(\mathbf{U})$ and $C_2 = C_2(\mathbf{U})$. In practice,the parameter $\epsilon > 0$ is take to be arbitrarily small and, clearly, setting ϵ to 0 reduces (1.3) to the hyperbolic system (1.1). Furthermore, the parameter α plays a fundamental role in the theory of shock waves and measures the relative effect of dispersion and diffusion in the material.

In many systems of conservation laws, the entropy inequality (1.2) is consistent with (1.3) and encodes enough information about the small-scale effects so that the system (1.1) and the inequality (1.2) are sufficient to characterize a unique solution for every choice of initial data at $t = 0$. In particular, the entropy solution of (1.1) is independent of the underlying small-scale effects modeled by B, C_1, C_2 in (1.3). Different choices of regularizations yield the same limit solution as $\epsilon \to 0$.

On the other hand, there exist many interesting classes of models where the shock waves are *small-scale dependent* i.e, the solutions to the conservation law (1.1), realized as limits of the regularized diffusive-dispersive equation (1.3), depend explicitly on the regularizing terms B, C_1, C_2. Different regularizations can lead to different solutions for the conservation law. For this theory of nonclassical shocks to nonlinear hyperbolic systems, we refer to the review texts [26, 27, 28] and the references therein.

Such small-scale dependent shock waves can arise in a wide variety of systems of PDE's:

- *Nonconvex hyperbolic systems.* The examples of particular interest include the scalar conservation law with cubic flux with viscosity and capillarity terms (see (2.1, below), a reduced model from magnetohydrodynamics with Hall effect (see (4.2), below), and the van der Waals fluids with viscosity and capillarity (see (3.2), below).
- *Nonconservative hyperbolic systems:* These systems are of the form:

$$\mathbf{U}_t + A(\mathbf{U})\mathbf{U}_x = 0$$

  , where the matrix-valued $A = A(\mathbf{U})$ need not be a Jacobian matrix. Examples are coupled Burgers-like equations, Lagrangian gas dynamics with internal energy taken as an independent variable, and the multi-layer shallow water system. (See [5, 6] and the references therein.)
- *Boundary value problems.* Examples include both linearized and nonlinear Euler equations with artificial viscosity and with physical viscosity (of Navier-Stokes type). (See [21, 36] and the references therein.)

All the models of interest do possess an entropy inequality like (1.2), but such an entropy inequality fails to single out a physically relevant solution and further admissibility criteria are needed beyond the classical shock wave theory, specifically:

- For nonconvex hyperbolic systems that include capillarity, Hall effect, etc.,one needs a *kinetic function* in the sense of Hayes-LeFloch [19], which provides the rate of entropy dissipation across shocks. This notion was introduced first for a system arising in in material science by Abeyaratne and Knowles [1] and Truskinovsky [41], motivated by pioneering work by Slemrod [37] on viscosity-capillarity flows.
- For nonconservative hyperbolic systems, one needs a *family of paths* in the sense of Dal Maso-LeFloch-Murat [13], which represents a selection of an integration path in order to determine a generalized jump relation at shocks [24]. This notion can be seen as a vast generalization of the so-called Volpert's product [42, 23].

- For boundary value problems, a *set of admissible boundary states* in the sense of Dubois-LeFloch [14], which describes the jump between the prescribed boundary data and the actual boundary trace of solutions.

1.3. Numerical approximation of classical shocks. Numerical schemes approximating systems of conservation laws have undergone extensive development over the past three decades. Among the most popular discretization frameworks are the so-called finite difference methods and finite volume methods. (Cf. the textbook by LeVeque [34].) In these approaches, the point values or cell averages (of the unknown in (1.1)) are evolved at each time step in terms of differences of fluxes across cell interfaces. These fluxes are computed by using exact or approximate Riemann solvers of the Godunov, Lax-Friedrichs, or Harten-Lax-van Leer type. High-order spatial accuracy is obtained by using non-oscillatory, piecewise polynomial reconstructions of the TVD (total variation diminishing), ENO (ennsentially non-oscillatory) and WENO (weighted) type. An alternative approach relies on the so-called discontinuous Galerkin finite element method. Time integration can be performed with strong stability-preserving Runge-Kutta methods. These now classical frameworks have proven to be very successful in resolving most complex fluid flows modeled by hyperbolic systems of conservation laws (1.1).

1.4. Numerical approximation of small-scale dependent shocks. However, the standard finite difference (volume) schemes have not been successful in computing small-scale dependent shock waves. As an illustrative example, we consider here a cubic conservation law (see (2.1), below, for details)) with vanishing diffusion and capillarity and let us approximate its solutions with the help of the standard (first-order) Lax-Friedrichs and Rusanov schemes. The numerical results are shown in Figure 1.1.

The figure clearly shows that both the Lax-Friedrichs and Rusanov schemes completely fail to approximate the nonclassical shock for this scalar conservation law. In fact, any other monotone scheme, such as the Godunov and Engquist-Osher schemes also fail to resolve the nonclassical shock in this case. The failure of standard schemes

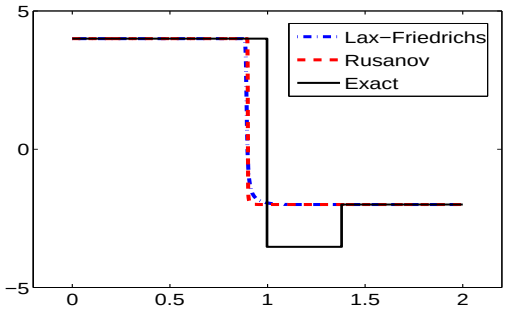

FIG. 1.1. *Approximation of small-scale dependent shock waves for the cubic conservation law with vanishing diffusion and capillarity using the standard Lax-Friedrichs and Rusanov schemes*

to approximate small-scale dependent shock waves accurately has been well documented for nonclassical shocks (cf. [18] and subsequent papers [8, 10, 32]) and subsonic phase boundaries as well as in other contexts such as in nonconservative hyperbolic systems (cf. [20] and subsequent papers[2, 4, 5, 6, 7, 16]) and in boundary value problems (cf. [36]).

We do not try to review here the extensive literature on the numerical approximation of small-scale dependent shocks, but refer the reader to the forthcoming review [31].

This failure of standard schemes in approximating small-scale dependent shock waves in various contexts can be explained in terms of the equivalent equation of the scheme (as first observed in [20, 18, 36] for nonconservative, nonconvex, and boundary problems, respectively). As is well-known, the equivalent equation represents the role of (mesh-dependent) higher-order terms (derivatives) and it typically of the following form for a first-order scheme,

$$\mathbf{U}_t + \mathbf{F}(\mathbf{U})_x = \Delta x(\overline{B}(\mathbf{U})\mathbf{U}_x)_x + \alpha\Delta x^2(\overline{C}_1(\mathbf{U})(\overline{C}_2(\mathbf{U})\mathbf{U}_x)_x)_x + \mathcal{O}(\Delta x^3). \tag{1.4}$$

Standard schemes are often such that $\overline{B} \neq B$, $\overline{C}_1 \neq C_1$, and $\overline{C_2} \neq C_2$, with $B, C_{1,2}$ prescribed by the physical model (1.3). As the small-scale dependent shock waves, realized as the $\epsilon \to 0$ limit of (1.3), depend explicitly on the expressions of the diffusion and dispersion terms, this difference in the diffusion and dispersion terms between (1.4) and (1.3) is the *crucial* reason as to why standard schemes fail to correctly approximate small-scale dependent shock waves.

The equivalent equation provides a suitable tool for constructing schemes that are better at approximating small-scale dependent shock waves. The key idea is to design finite difference schemes whose equivalent equation can match (1.3) for both the diffusive and dispersive terms. These schemes are designed such that $\overline{B} = B$, $\overline{C}_{1,2} = C_{1,2}$ in their equivalent equation (1.4). Such schemes have been proposed in the above cited references.

As an example, consider the scheme proposed in [32] for approximating the scalar cubic conservation law (2.1). As shown in Figure 1.2 (left), this scheme is quite effective in computing the nonclassical shock wave. However, the effectiveness of this scheme deteriorates when the shock strength is increased. This phenomenon is also illustrated in 1.2 (center and right). As shown in the figure, for larger shock strengths, particularly for the one with a jump of around 20 at the nonclassical shock, these schemes fail to approximate nonclassical shocks with *large* amplitude. Similar failure to approximate strong shocks has also been documented for nonconservative hyperbolic systems [20, 7] and boundary value problems [36]. This failure of finite difference schemes to approximate small-scale dependent shock waves of arbitrary strength has been an outstanding open problem in this context.

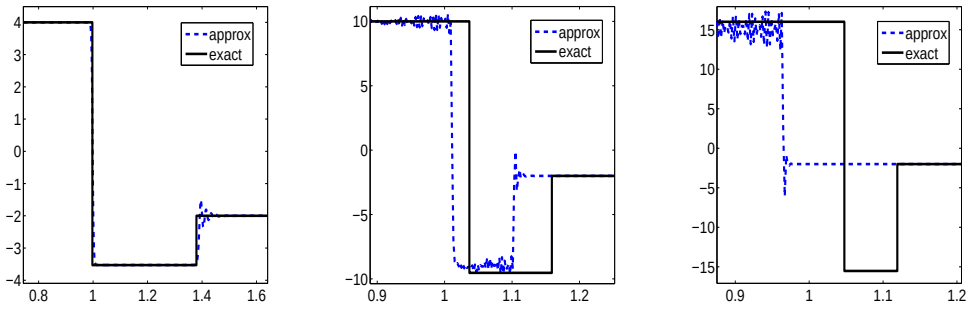

FIG. 1.2. *Approximation of nonclassical shocks for the cubic conservation law with leFloch-Mohamadian's scheme. Left: Initial Jump* 4. *Center: Initial jump* 10. *Right: Initial jump* 16.

1.5. Aims of this paper. Our main objective here is to propose a new class of finite difference schemes, which can approximate nonclassical shock waves for non-convex hyperbolic systems of conservation laws correctly for any underlying shock strength. In particular, nonclassical shocks of arbitrary strength can be efficiently and correctly approximated with our approach. The follow-up work [3] will develop this strategy for nonconservative and boundary problems as well.

The key design principle still relies on the *equivalent equation* (1.4). We identify here the main reason as to why a scheme which has an equivalent equation of the form (1.4), even with matching diffusion and dispersion operators, may fail to approximate strong nonclassical shocks correctly. It lies in the higher-order terms (i.e $\mathcal{O}(\Delta x^3)$ and higher) of the equivalent equation. For small enough shock strengths, these terms are insignificant in comparison to the flux term and the leading-order terms (the diffusion and dispersion terms) of the equivalent equation. However, as the shock strength is increased, the higher-order terms become as significant and even more significant in amplitude than the leading order terms and can drive the dynamics of the scheme. This issue is clearly highlighted quantitively in illustrative test cases presented below.

Our analysis also suggests that the appropriate design principle for constructing finite difference schemes to approximate nonclassical shocks correctly is to ensure the following conditions:

- The leading order terms of the equivalent equation of the finite difference scheme match the appropriate diffusion and dispersion operators in (1.3).
- The higher-order terms ($\mathcal{O}(\Delta x^3)$ and higher) of the equivalent equation remain *small* in comparison to the leading order terms, particularly for strong shocks.

We propose to term such a class of finite difference schemes as schemes with *well-controled diffusion (WCD)*. The rest of the paper is devoted to presenting and testing such schemes. The WCD condition is imposed by choosing *time-dependent* numerical diffusion and dispersion coefficients. Sufficient conditions are identified for sufficiently high-order schemes for any given user specified tolerance by which the higher-order terms in the equivalent equation are controlled in terms of low-order terms. Numerical experiments show that the WCD schemes indeed approximate nonclassical shock waves of arbitrarily large amplitude very accurately.

The paper is organized as follows: in Section 2, we consider scalar conservation laws with linear diffusion and dispersion and we present a class of WCD schemes to approximate its nonclassical solutions. In Section 3, a class of WCD scheme is presented for systems of conservation laws and is then specialized to the dynamics of van der Waals fluids and a simplified model of magnetohydrodynamics. Extensive numerical experiments illustrating the power and performance of WCD schemes are presented in both sections.

2. WCD schemes for scalar conservation laws.

2.1. Kinetic function for the cubic flux. To start with, we consider fscalar conservation laws with vanishing diffusion and capillarity, that is,

$$u_t + f(u)_x = \epsilon u_{xx} + \delta\, \epsilon^2 u_{xxx}. \tag{2.1}$$

For non-convex flux-functions f and, for instance, $f(u) = u^3$, and when $\delta \neq 0$, the limiting solutions (as $\epsilon \to 0$) of the resulting conservation law

$$u_t + f(u)_x = 0 \tag{2.2}$$

may contain *nonclassical shocks*, as described in [27, Chap. 2]. The nonclassical Riemann solution is determined from a kinetic function $\varphi^\flat : \mathbf{R} \to \mathbf{R}$, which in the case of the cubic flux (and the entropy $U = u^2/2$) satisfies the fundamental inequalities,

$$-u^2 < u\,\varphi^\flat(u) \le -u^2/2, \qquad u \in \mathbf{R}.$$

A kinetic function, by definition, is a monotone non-increasing function satisfying these inequalities and, in the case of the regularization (2.1). It is explicitly given by

$$\begin{aligned} \varphi^\flat(u) &= -u \pm \sqrt{2\delta}/3, \quad \pm u \ge \sqrt{2\delta}/3, \\ \varphi^\flat(u) &= -u/2, \qquad |u| \le \sqrt{2\delta}/3. \end{aligned}$$

The kinetic relation serves to uniquely characterize the nonclassical solutions to the cubic conservation law. Our aim is to numerically approximate the nonclassical shocks in an accurate and efficient manner.

2.2. WCD schemes for scalar conservation laws. Consider a discretization $[x_i, x_{i+1})$ of the domain of interest $[a, b]$ into points $\{x_i\}$ with uniform (for simplicity) mesh width $x_{i+1} - x_i = \Delta x > 0$. For any integer $p \ge 1$, we approximate (2.2) with the following $2p$-th order consistent finite difference scheme:

$$\frac{du_i}{dt} + \frac{1}{\Delta x} \sum_{j=-p}^{j=p} \alpha_j f_{i+j} = \frac{c}{\Delta x} \sum_{j=-p}^{j=p} \beta_j u_{i+j} + \frac{\delta c^2}{\Delta x} \sum_{j=-p}^{j=p} \gamma_j u_{i+j}. \tag{2.3}$$

Here, $u_i(t) \approx u(x_i, t)$ is the cell nodal value, $f_i = f(u_i)$ is the flux, the constant δ is the coefficient of capillarity (given by the physics of the problem) and $c = c(t) \ge 0$ will be determined later on. The coefficients α_j, β_j and γ_j need to satisfy the following *$2p$-order conditions*:

$$\sum_{j=-p}^{p} j\alpha_j = 1, \qquad \sum_{j=-p}^{p} j^l \alpha_j = 0, \qquad l \ne 1, \quad 0 \le l \le 2p. \tag{2.4}$$

Observe that (2.4) defines a set of $(2p+1)$ linear equations for $(2p+1)$ unknowns and can be solved explicitly. Similarly, the coefficients β must satisfy

$$\sum_{j=-p}^{p} j^2\beta_j = 2, \qquad \sum_{j=-p}^{p} j^l \beta_j = 0, \qquad l \ne 2, \qquad 0 \le l \le 2p \tag{2.5}$$

while, for the coefficients γ,

$$\sum_{j=-p}^{p} j^3\gamma_j = 6, \qquad \sum_{j=-p}^{p} j^l \gamma_j = 0, \qquad l \ne 3, \qquad 0 \le l \le 2p. \tag{2.6}$$

Some remarks about the finite difference scheme (2.3) are in order:

- The scheme (2.3) is a conservative and consistent discretization of the conservation law (2.2). It is formally only first-order accurate since the diffusive terms are proportional to Δx. The scheme need not preserve the monotonicity of the solutions.
- The scheme (2.3) is not entropy stable with respect to the quadratic entropy $S(u) = \frac{u^2}{2}$ as the numerical flux discretization is not entropy conservative (in the sense of Tadmor [38, 39]). However, it is straightforward to design a $2p$-th order accurate version that is entropy conservative as in [29, 30].

2.3. Equivalent equation near a shock. The equivalent equation associated with the finite difference scheme (2.3) reads

$$\frac{du}{dt} + f(u)_x = c\Delta x\, u_{xx} + \delta c^2 (\Delta x)^2\, u_{xxx} - \sum_{k=2p+1}^{\infty} \frac{(\Delta x)^{k-1}}{k!} A_k^p (f(u))^{[k]} + c \sum_{k=2p+1}^{\infty} \frac{(\Delta x)^{k-1}}{k!} B_k^p u^{[k]} + \delta c^2 \sum_{k=2p+1}^{\infty} \frac{(\Delta x)^{k-1}}{k!} C_k^p u^{[k]}. \tag{2.7}$$

Here, $g^{[k]} = \frac{d^k g}{dx^k}$ denotes the k-th spatial derivative of a smooth function g and the coefficients above are given by

$$A_k^p = \sum_{j=-p}^{p} \alpha_j j^k, \qquad B_k^p = \sum_{j=-p}^{p} \beta_j j^k, \qquad C_k^p = \sum_{j=-p}^{p} \gamma_j j^k, \tag{2.8}$$

with α, β and γ being specified by the relations (2.4), (2.5), and (2.6), respectively.

Assume that we have a single shock connecting some states u_L and u_R such that $[\![u]\!] = u_L - u_R > 0$ and $[\![f(u)]\!] > 0$ (the other cases being handled similarly). At this shock, we formally find

$$u^{[k]} \simeq \frac{[\![u]\!]}{\Delta x^k}, \qquad (f(u))^{[k]} \simeq \frac{[\![f(u)]\!]}{\Delta x^k}.$$

Substituting these formal relations into the equivalent equation (2.7) at a single shock, we obtain

$$\frac{du}{dt} + \underbrace{\frac{[\![f(u)]\!]}{\Delta x} - \frac{c[\![u]\!]}{\Delta x} - \frac{\delta c^2 [\![u]\!]}{\Delta x}}_{l.o.t} \simeq \underbrace{\frac{S_p^D c[\![u]\!]}{\Delta x} + \frac{S_p^C \delta c^2 [\![u]\!]}{\Delta x} - \frac{S_p^f [\![u^3]\!]}{\Delta x}}_{h.o.t} \tag{2.9}$$

Here, the coefficients are given by

$$S_p^f = \sum_{k=2p+1}^{\infty} \frac{A_k^p}{k!}, \qquad S_p^D = \sum_{k=2p+1}^{\infty} \frac{B_k^p}{k!}, \qquad S_p^C = \sum_{k=2p+1}^{\infty} \frac{C_k^p}{k!}, \tag{2.10}$$

with A_k^p, B_k^p, C_k^p being defined in (2.8).

The relation (2.9) represents the balance of terms in the equivalent equation in the neighborhood of a single shock. Ideally, the higher-order error terms (h.o.t in (2.9)) should be dominated in amplitude by the leading-order terms (l.o.t in (2.9)).

2.4. The WCD condition. We seek to balance both sets of terms through a user-defined tolerance parameter $\tau << 1$. In order words, we impose the condition $\frac{|h.o.t|}{|l.o.t|} < \tau$, which we ensure by a comparing, one one hand, the upper bound

$$|h.o.t| \leq \left(\hat{S}_p^D c + \hat{S}_p^C |\delta| c^2 + \hat{S}_p^f \sigma \right) \frac{|[\![u]\!]|}{\Delta x},$$

where $\sigma = \frac{|[\![f(u)]\!]|}{|[\![u]\!]|}$ denotes the amplitude of the shock speed and

$$\hat{S}_p^f = \sum_{k=2p+1}^{\infty} \left| \sum_{j=-p}^{p} \frac{\alpha_j j^k}{k!} \right|, \; \hat{S}_p^D = \sum_{k=2p+1}^{\infty} \left| \sum_{j=-p}^{p} \frac{\beta_j j^k}{k!} \right|, \; \hat{S}_p^C = \sum_{k=2p+1}^{\infty} \left| \sum_{j=-p}^{p} \frac{\gamma_j j^k}{k!} \right|, \tag{2.11}$$

with, on the other hand, the lower bound

$$|l.o.t| \geq \left(|\delta|c^2 + c - \sigma\right) \frac{|[\![u]\!]|}{\Delta x}.$$

Thus, we achieve the condition $\frac{|h.o.t|}{|l.o.t|} < \tau$ *provided*

$$(2.12) \qquad (\mathbf{WCD}): \quad \left(|\delta| - \frac{\hat{S}_p^C|\delta|}{\tau}\right) c^2 + \left(1 - \frac{\hat{S}_p^D}{\tau}\right) c - \left(1 + \frac{\hat{S}_p^f}{\tau}\right) \sigma > 0,$$

which we refer to as the *WCD condition* for the proposed class of schemes. Recall that τ is a user-defined tolerance, δ is the coefficient of dispersion, $\hat{S}_P^{f,D,C}$ are specified in (2.11) and can be precomputed before the actual numerical simulation, while σ is the shock speed (of the shock connecting u_L and u_R) and depends on the solution under consideration. The only genuine parameter to be chosen is the numerical dissipation coefficient c. This coefficient must be evaluated at each time step and chosen to satisfy the WCD condition (2.12)

The crucial question is whether there exists a suitable c such that the WCD condition (2.12) is satisfied for a given p. Given the above framework, elementary properties of Vandermonde determinants (as observed by Dutta [15]) imply that the coefficients $\hat{S}_p^{f,D,C}$ satisfy

$$(2.13) \qquad \lim_{p \to +\infty} \max\{\hat{S}_p^f, \hat{S}_p^D, \hat{S}_p^C\} = 0.$$

Our numerical experiments overwhelmingly demonstrate this property and, moreover, the quantities decay algebraically, as illustrated in Figure 2.1.

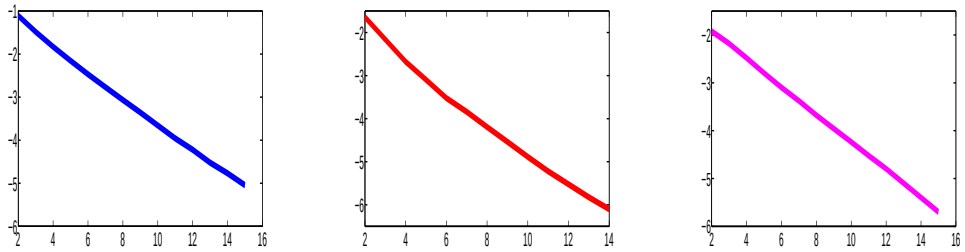

FIG. 2.1. *Decay of the coefficients* $\hat{S}_p^{f,D,C}$ *with increasing p. Left: p (X-axis) vs.* $\log_{10}(\hat{S}_p^f)$ *(Y-axis). Middle: p (X-axis) vs.* $\log_{10}(\hat{S}_p^D)$ *(Y-axis) Right: p (X-axis) vs.* $\log_{10}(\hat{S}_p^C)$ *(Y-axis).*

As c is a coefficient of diffusion in (2.3), we need that $c > 0$. A simple calculation with the quadratic relation (2.12) shows that $c > 0$ if and only if

$$(2.14) \qquad \frac{\hat{S}_p^C}{\tau} < 1,$$

as σ (being the absolute value of the shock speed) is always positive.

Given (2.13), we can always find a large enough p such that the sufficient condition (2.14) is satisfied for any given tolerance τ. Hence, the "order" of the finite difference scheme (2.3) needs to be increased in order to control the high-order terms in the equivalent equation, in terms of the leading order terms.

Furthermore, in the limit of infinite p and for any $\tau > 0$, the above lemma will imply the following limiting **WCD** condition:

$$|\delta|c^2 + c - \sigma > 0. \tag{2.15}$$

Solving the quadratic equation explicitly yields two real roots, one being negative and the other one positive. The convexity of the function implying that choosing $c > c_2$, with c_2 being the positive root of the above quadratic equation. Thus for large enough p (higher-order schemes), we can always choose a suitable numerical dissipation coefficient (depending on both δ and the wave speed σ) that yields the correct small-scale dependent shock waves.

Finally, we easily extend the above analysis at a single shock and determine the diffusion coefficient c in the finite difference scheme (2.3) in the following manner. First, at each interface $x_{i+1/2} = \frac{1}{2}(x_i + x_{i+1})$, we use $u_L = u_i$ and $u_R = u_{i+1}$ in the WCD condition (2.12) and choose a coefficient $c_{i+1/2}$ such that this condition is satisfied. Then, the coefficient for the entire scheme is given by

$$c := c(t) = \max_i c_{i+1/2}. \tag{2.16}$$

2.5. Shocks of small, moderate, or large strength. In the rest of this section, we test the WCD schemes (2.3) on a series of relevant examples. We consider the cubic conservation law i.e, (2.2) with $f(u) = u^3$ and, for definiteness, we set $\delta = 1$ in (2.1). As the finite difference schemes (defined above) are semi-discrete, we integrate in time using a third-order strong stability preserving Runge-Kutta time stepping method. The time step is determined using a standard CFL condition with CFL number being 0.45 for all numerical experiments, which we have checked to be sufficient for our purpose in the present paper.

For determining the coefficient c, we need to choose τ as well as the order $2p$ of the scheme and then compute the dissipation coefficient suggested by the WCD condition. We use here the following Riemann initial data

$$u(0, x) = u_L \quad \text{if} \quad x < 0.4; \qquad -2, \quad \text{if} \quad x > 0.4.$$

We vary u_L and consider three different regimes, namely:

- *Small shocks*: The maximum shock strength is less that 10.
- *Moderate shocks*: The maximum shock amplitude is between 10 and 100.
- *Large shocks*: The maximum strength is greater than 100.

2.5.1. Small shocks. We consider two different sets of $u_L = 2$ and $u_L = 4$ to represent small shocks. The numerical results are presented in Figure 2.2. In this figure, we present approximate solutions for both sets of initial data, computed with a eighth-order WCD scheme and with $\tau = 0.01$ on a sequence of meshes. For $u_L = 2$, we see that the WCD scheme is able to approximate the nonclassical shock wave, preceded by a rarefaction wave. Similarly for $u_L = 4$, we see that the WCD scheme approximates both the leading classical shock wave and the trailing nonclassical shock wave quite well. In both cases, the quality of approximation improves on mesh refinement. As expected, there are some oscillations at the leading shock. This is on account of the dispersive terms in the equivalent equation. As mentioned before, schemes presented in [32] were also able to compute small shocks (here the maximum shock strengh is around 7) quite well. So, it is not surprising that the WCD scheme is able to perform quite well. Since the other WCD schemes (of order 4 and higher) performed equally well (for different choices of τ), we omit the results with those schemes.

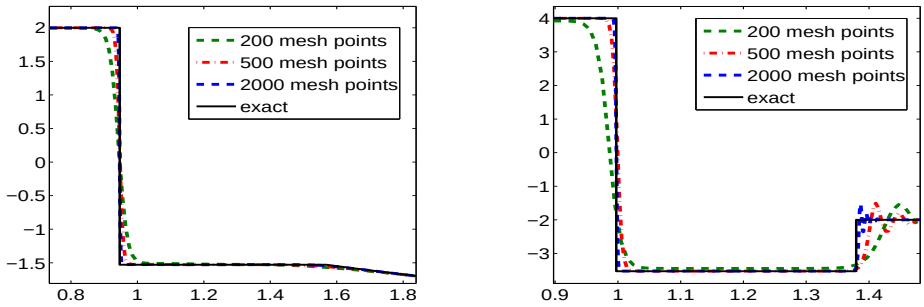

FIG. 2.2. *Convergence (mesh refinement) for the WCD scheme on small shocks. All approximations are based on an order* 8 *scheme and* $\tau = 0.01$. *Left: Solution of the Riemann problem for* $u_L = 2$. *Right: Solution of the Riemann problem for* $u_L = 4$.

2.5.2. Moderate shocks. In order to simulate nonclassical shocks of moderate strength, we consider $u_L = 30$ and present numerical results in Figures 2.3 and 2.4. The exact solution in this case consists of a leading shock and a trailing nonclassical shock of strength or around 60 (far stronger than the previous experiment and the results presented in [32]). In Figure 2.3, we illustrate how WCD schemes of different order approximate the solution for 4000 mesh points. A related issue is the variation of the parameter τ. Observe that τ represent how strong the high-order terms are allowed to be vis a vis the leading order diffusion and dispersion terms. Also, the order of the scheme depends on the choice of τ. For instance, choosing $\tau = 0.1$ implies that fourth-order schemes ($p = 2$) are no longer consistent with the WCD condition (2.12) for this choice of τ and one has to use a *sixth-* or even higher order scheme. In this particular experiment, we choose $\tau = 0.3$ (fourth-order scheme), $\tau = 0.1$ (eighth-order) scheme and $\tau = 0.01$ (twelfth-order) scheme. As shown in Figure 2.3, all the three schemes approximate the nonclassical shock quite well. There are some dispersive oscillations at the leading shock and in the intermediate state. It is observed that increasing the order of the schemes only leads to a minor improvement in the quality of the results. Also, increasing τ did not severely affect the shock-capturing abilities of the scheme. Clearly, the eighth and twelfth-order schemes were slightly better in this problem. The results should be contrasted to Figure 1.2 where schemes proposed in [32] (atleast for a certain choice of parameters) were unable to approximate even jumps of around 20. In this example, the WCD schemes were able to approximate jumps of a much larger magnitude quite efficiently.

In Figure 2.4, a different moderate shock, initialized with $u_L = 25$ and computed with an eighth-order scheme is shown. The results clearly show that the scheme converges to the correct nonclassical solution with increasing mesh refinement. As expected, there are oscillations (with increasing frequency for finer mesh resolutions) at the leading shock. However, properties such as the intermediate state and the shock speeds (for both the classical and nonclassical shocks) are correctly approximated, even at coarse mesh resolutions. Similar results were also obtained with the fourth and twelfth-order schemes.

2.5.3. Large shocks. Finally, we simulate a very strong shock using $u_L = 55$ in the initial data. The numerical results are presented in Figure 2.5. The exact solution consists of a strong nonclassical shock of magnitude around 110 and a weaker (but still

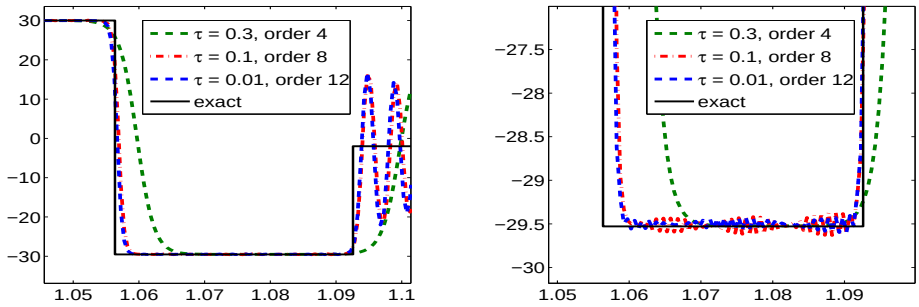

FIG. 2.3. *Convergence $p \to +\infty$ (increasing order of the scheme) for the WCD scheme for a moderate shock. Left: Solution of the Riemann problem for $u_L = 30$. Right: Closer view of the middle state u_M.*

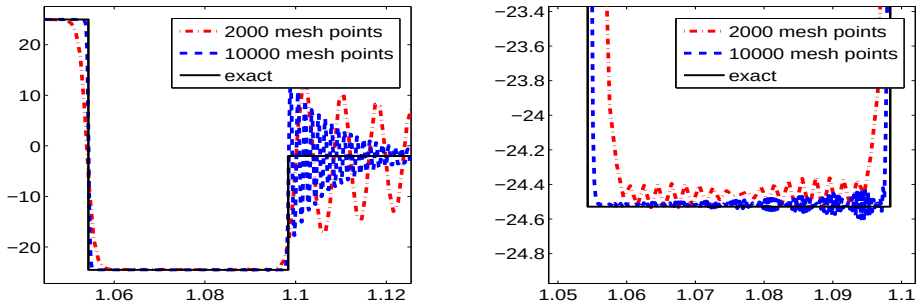

FIG. 2.4. *Mesh refinement for a moderate shock with an eighth-order WCD scheme. Left: Solution of the Riemann problem for $u_L = 25$. Right: Closer view of the middle state u_M.*

of amplitude 60) leading shock wave. The results in the figure were generated with the fourth, eighth and twelfth order schemes. The mesh resolution is quite fine (20000 mesh points) as the difference in speeds for both shocks is quite small, the intermediate state is very narrow and needs to be resolved. It is important to emphasize that one can easily use a grid, adapted to the shock locations. The results clearly show that all the three schemes converge to the correct nonclassical shock, even for such a strong shock.

2.6. Computing the kinetic relation. According to the general theory of nonclassical entropy solutions [27], nonclassical shocks can be uniquely characterized in terms of a *kinetic relation*, which relates the entropy dissipation across the nonclassical shock. This characterization is provided by the specification of the right-hand states connected to each left-hand state via a nonclassical shock. Since, the exact intermediate state of a Riemann problem is known for the cubic conservation law (for any given value of the dispersion parameter δ), we can ascertain the quality and accuracy of numerical approximation for a very large class of initial data by computing the numerical kinetic relation. We do so using the eighth-order WCD scheme for three different values of the dispersion parameter δ. The results are presented in Figure 2.6 and clearly demonstrate that this WCD scheme is able to compute the correct intermediate state (kinetic relation) and hence, the nonclassical shock wave, accurately for

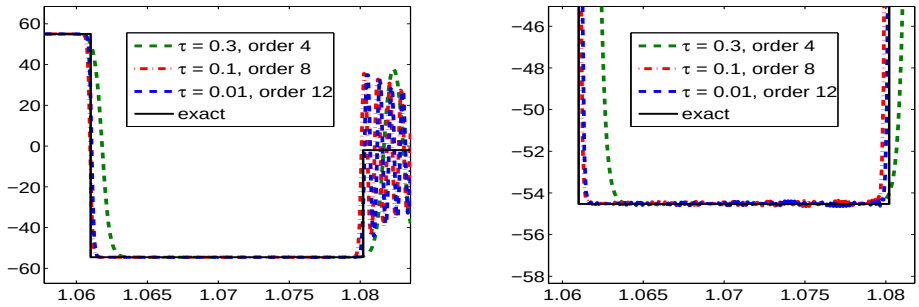

FIG. 2.5. *Convergence $p \to +\infty$ for a large nonclassical shock for the cubic conservation law. Left: Solution of the Riemann problem for $u_L = 55$. Right: Closer view of the middle state u_M.*

any given shock strength. In particular, very strong nonclassical shocks are captured accurately. Similar results were also obtained with WCD schemes of different orders.

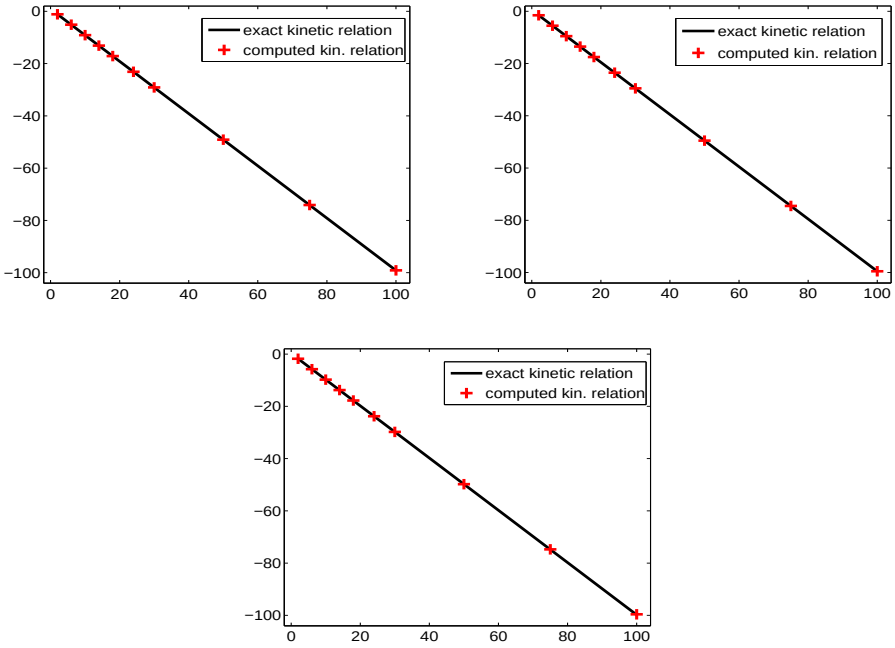

FIG. 2.6. *Intermediate state (kinetic function) (Y-axis) for the cubic conservation law for varying left state $u - L$ (X-axis), computed using an eighth-order WCD scheme with $\tau = 0.1$. Left: Kinetic function for $\delta = 0.3$. Middle: Kinetic function for $\delta = 1$. Right: Kinetic function for $\delta = 5$.*

2.7. Sharpness of the WCD condition. We have seen in the above numerical experiments that finite difference schemes that obey the WCD condition (2.12) are able to accurately approximate nonclassical shocks, independent of the underlying shock strength. The WCD condition itself has been obtained using orders-of-magnitude analysis and it is difficult to determine whether the WCD constant, as

specified from the quadratic equation (2.12), is sharp or not. At the very least, one would expect that violating the WCD condition by a considerable extent will impede the ability of a finite difference scheme to accurately approximate a nonclassical shock wave. This hypothesis is tested in a numerical experiment with the initial left state being set to $u_L = 15$. The exact solution consists of a nonclassical shock wave of amplitude of approximately 30 and a leading shock wave. As expected, the eighth-order finite difference scheme with $\tau = 0.1$ is clearly able to approximate this solution when the diffusion coefficient c is set to be exactly the larger (positive) root of the quadratic equation in the WCD condition (2.12). On the other hand, changing the value of c such that $c = 0.25c_{wcd}$ and thus violating the WCD condition to a significant extent, the same scheme is no longer able to approximate the correct shock waves. This experiment clearly illustrates that although the WCD condition may not be completely sharp, it may be necessary to scale the diffusion and dispersion terms of the scheme using it in order to approximate nonclassical shock waves.

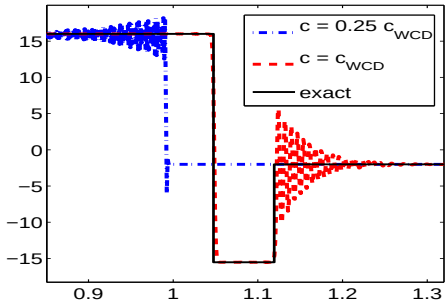

FIG. 2.7. *Approximation of a nonclassical shock for the cubic conservation law with left state* $u_L = 15$*, with the eighth-order WCD scheme for* $c = 0.25c_{WCD}$ *(blue)* not *satisfying the WCD condition (2.12) and for* $c = c_{WCD}$ *(red) satisfying (2.12)*

3. WCD schemes for systems: van der Waals fluids. In this and the following section, we will consider systems of conservation laws that can have small-scale dependent shock waves as solutions. For the sake of simplicity, we focus on two very general and frequently occurring subcases namely,

3.1. Van der Waals fluids with viscosity and capillarity. The system of conservation laws with viscosity and capillarity is given by

$$\mathbf{U}_t + \mathbf{F}_x = \epsilon D^{(1)}\mathbf{U}_{xx} + \alpha\epsilon^2 D^{(2)}\mathbf{U}_{xxx}, \tag{3.1}$$

where $\mathbf{U}$ is the vector of unknowns, $\mathbf{F}$ the flux vector and D^1, D^2 are viscosity and capillarity matrices, respectively.

As a concrete example of systems of conservation laws with viscosity and capillarity, we consider the following two conservation laws:

$$\begin{aligned} \tau_t - u_x &= 0, \\ u_t + p(\tau)_x &= \epsilon u_{xx} - \alpha\,\epsilon^2 \tau_{xxx}. \end{aligned} \tag{3.2}$$

Here, u and τ represent the velocity and the specific volume of the fluid, respectively, while α is a non-negative parameter representing the strength of the capillarity. We

consider an equation of state for van der Waals-type fluids, described by the (normalized) equation

$$p(\tau) := \frac{1}{(3\tau-1)^{1+1/\zeta}} - \frac{3}{\tau^2}, \quad u > 1/3, \tag{3.3}$$

for some positive constant $\zeta = 1/(\gamma-1)$ where $\gamma \in (1,2)$. The pressure law $p = p(\tau) > 0$ is defined for all $\tau \in (0,+\infty)$ and there exist $0 < a < c$ such that

$$\begin{aligned} p''(\tau) > 0, \quad \tau \in (0,a) \cup (c,+\infty), \\ p''(\tau) < 0, \quad \tau \in (a,c), \qquad\qquad p'(a) > 0, \end{aligned}$$

and, clearly, $\lim_{\tau\to 0} p(\tau) = +\infty$ while $\lim_{\tau\to+\infty} p(\tau) = 0$.

Under these conditions, the above system forms a first-order system of partial differential equations, which is of elliptic type when τ belongs in the interval (d,e) characterized by the conditions $0 < d < a < e < c$ and $p'(d) = p'(e) = 0$. It is of hyperbolic type when $\tau \in (0,d) \cup (e,+\infty)$ and admits the two (distinct, real) wave speeds $\pm\sqrt{-p'(\tau)}$.

Observe that the above system can be recast in the general form (3.1) with

$$\mathbf{U} = \begin{pmatrix} \tau \\ u \end{pmatrix}, \qquad D^{(1)} = \begin{pmatrix} 0 & 0 \\ 0 & 1 \end{pmatrix}, \qquad D^{(2)} = \begin{pmatrix} 0 & 0 \\ -1 & 0 \end{pmatrix}$$

and the flux vector $\mathbf{F} : R^2 \to R^2$ is given by $\mathbf{F}(\tau,u) = \begin{pmatrix} -u \\ p(\tau) \end{pmatrix}$. It is well-known that solutions to this model may contain nonclassical shocks. However, the existence of kinetic relations for characterizing these shocks has not been rigorously established yet.

3.1.1. WCD schemes for systems of conservation laws. We consider a grid as in the previous section on scalar equations. A $2p$-th order accurate finite difference scheme for approximating (3.1) is given by

$$\begin{aligned} &\frac{d\mathbf{U}_i}{dt} + \frac{1}{\Delta x}\sum_{j=-p}^{j=p} \alpha_j \mathbf{F}_{i+j} \\ &= \frac{c}{\Delta x}\sum_{j=-p}^{j=p} \beta_j D^{(1)}\mathbf{U}_{i+j} + \frac{\delta c^2}{\Delta x}\sum_{j=-p}^{j=p} \gamma_j D^{(2)}\mathbf{U}_{i+j}, \end{aligned} \tag{3.4}$$

where $\mathbf{U}_i = \mathbf{U}(x_i,t)$, $\mathbf{F}_i = \mathbf{F}(\mathbf{U}_i)$ and the coefficients α_j, β_j and γ_j need to satisfy the order conditions (2.4)-(2.6).

As in the section on scalar equations, the key tool in designing a scheme that can accurately approximate the nonclassical shocks of (3.1) is the equivalent equation of the scheme (3.4) given by

$$\begin{aligned} \frac{d\mathbf{U}}{dt} = &\underbrace{-\mathbf{F}_x + c\Delta x D^{(1)}\mathbf{U}_{xx} + \delta c^2 \Delta x^2 D^{(2)}\mathbf{U}_{xxx}}_{l.o.t} \\ &\underbrace{- \sum_{k=2p+1}^{\infty} \frac{\Delta x^{k-1}}{k!} A_k^p \mathbf{F}^{[k]} + c\sum_{k=2p+1}^{\infty} \frac{\Delta x^{k-1}}{k!} B_k^p D^{(1)}\mathbf{U}^{[k]} + \delta c^2 \sum_{k=2p+1}^{\infty} \frac{\Delta x^{k-1}}{k!} C_k^p D^{(2)}\mathbf{U}^{[k]}}_{h.o.t}. \end{aligned} \tag{3.5}$$

The coefficients A_k^p, B_k^p and C_k^p are defined as in (2.8).

As in the previous section, our design of a WCD scheme is based on analysis at a single shock. Adapted from the scalar case we impose a componentwise condition to balance high-order and low-order terms for the equivalent equation for a single shock. Assume that there exists a tolerance τ such that $|h.o.t.| \leq \tau\,|l.o.t.|$ holds componentwise. Performing a similar analysis as in subSection 2.3 we may impose an upper bound for the high-order terms given by the element-wise condition

$$|h.o.t| \leq \left(\hat{S}_p^D c_i |\left\langle D_i^{(1)}, [\![\mathbf{U}]\!]\right\rangle| + \hat{S}_p^C |\delta| c_i^2 |\left\langle D_i^{(2)}, [\![\mathbf{U}]\!]\right\rangle| + \hat{S}_p^f \sigma |[\![\mathbf{U}_i]\!]|\right), \qquad (i=1,2)$$

where $\hat{S}_p^D, \hat{S}_p^C, \hat{S}_p^f$ and σ are defined as in (2.11) and $\langle .,. \rangle$ is used to denote the dot product of two vectors and

$$\sigma = \frac{|[\![\mathbf{F}(\mathbf{U})]\!]|}{|[\![\mathbf{U}]\!]|}, \tag{3.6}$$

being an estimate on the maximum shock speed of the system,

Furthermore, a lower bound for the low-order terms is given by

$$|l.o.t| \geq \left(|\delta| c_i^2 |\left\langle D_i^{(2)}, [\![\mathbf{U}]\!]\right\rangle| + c_i |\left\langle D_i^{(1)}, [\![\mathbf{U}]\!]\right\rangle| - \sigma |[\![\mathbf{U}_i]\!]|\right) \qquad (i=1,2).$$

Combining the two bounds we may obtain the condition $|h.o.t.| \leq \tau\,|l.o.t.|$ by ensuring the two conditions

$$(\mathbf{WCD})_i: \quad \left(|\delta| - \frac{\hat{S}_p^C |\delta|}{\tau}\right) |\left\langle D_i^{(2)}, [\![\mathbf{U}]\!]\right\rangle| c_i^2 + \left(1 - \frac{\hat{S}_p^D}{\tau}\right) |\left\langle D_i^{(1)}, [\![\mathbf{U}]\!]\right\rangle| c_i - \left(1 + \frac{\hat{S}_p^f}{\tau}\right) \sigma |[\![\mathbf{U}_i]\!]| > 0 \tag{3.7}$$

simultaneously. Observe that if $\left\langle D_i^{(1)}, [\![\mathbf{U}]\!]\right\rangle = 0$, we set the corresponding $c_i = 0$ for $i = 1, 2$. The scheme parameter c in (3.4) is defined as $c = \max\limits_{i=1,2} c_i$.

We can easily extend this analysis at a single shock to determine the diffusion coefficient c in the finite difference scheme (3.4) in the following manner. First, at each interface $x_{i+1/2} = \frac{1}{2}(x_i + x_{i+1})$, we use $\mathbf{U}_L = \mathbf{U}_i$ and $\mathbf{U}_R = \mathbf{U}_{i+1}$ in the WCD condition (3.7) and choose a coefficient $c_{i+1/2}$ such that this condition is satisfied. Then, the coefficient for the entire scheme is given by $c := c(t) = \max_i c_{i+1/2}$.

3.2. Small, moderate, and large shocks in van der Waals fluids. In our numerical tests, we use the flux function in [32], given by

$$p(\tau) := \frac{RT}{(\tau - \frac{1}{3})} - \frac{3}{\tau^2}$$

with $R = \frac{8}{3}$ and $T = 1.005$ which has two inflection points at 1.01 and 1.85. Let $\alpha = 1$ and consider the initial Riemann data

$$u(x,0) = \begin{cases} 0.35 & x < 0.5 \\ 1.0 & x > 0.5 \end{cases} \qquad \tau(x,0) = \begin{cases} 0.8 & x < 0.5 \\ 2.0 & x > 0.5 \end{cases} \tag{3.8}$$

The scheme parameter is set to $c = c_{WCD}$. Figures 3.1 and 3.2 show a nonclassical state in both variables u and τ and displays mesh convergence of the scheme as the mesh is refined. Furthermore, the eighth-order WCD scheme approximates the nonclassical state quite well for both variables, even at a very coarse mesh resolution.

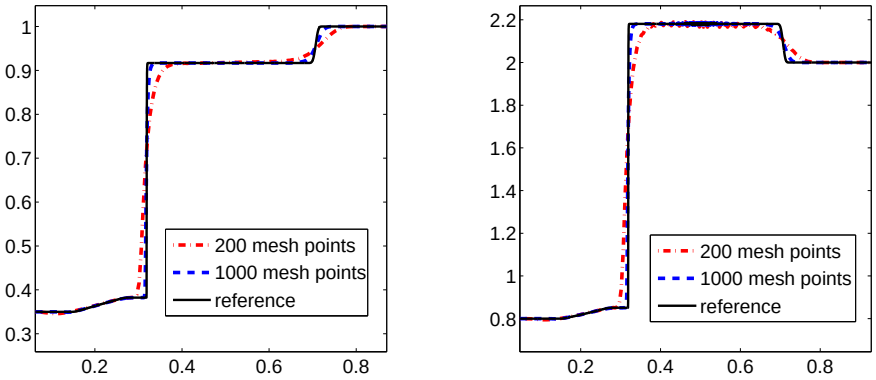

FIG. 3.1. *Mesh-convergence for the WCD scheme for the dispersive limit of van der Waals fluid with initial data (3.8) with a eighth-order WCD scheme. Left: Velocity u. Right: Volume τ.*

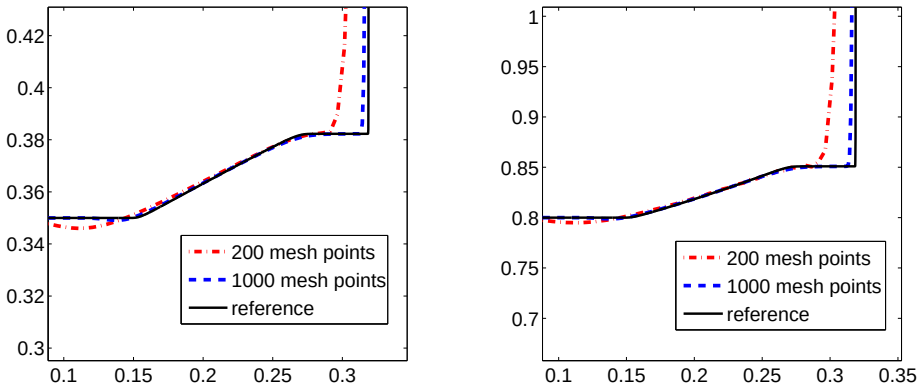

FIG. 3.2. *Zoom at the nonclassical states for the dispersive limit of van der Waals fluid with initial data (3.8) with a eighth-order WCD scheme. Left: Velocity u. Right: Volume τ.*

3.2.1. Large shocks. Next, we approximate large nonclassical shocks for a Van der Waals fluid by using the Riemann initial data

$$u(x,0) = \begin{cases} 0.35, & x < 0.5, \\ 1.5, & x > 0.5, \end{cases} \qquad \tau(x,0) = \begin{cases} 0.8, & x < 0.5, \\ 25.0, & x > 0.5. \end{cases} \tag{3.9}$$

The results with a eighth-order scheme are shown in figures 3.3 and 3.4 and clearly show that the WCD scheme is able to approximate the nonclassical shock of large amplitude (in the volume) quite well.

3.3. Violation of the WCD condition. As in the case of scalar conservation laws, the violation the WCD condition leads to situations where the nonclassical shocks are not approximated correctly. Furthermore, another interesting phenomena arises when the WCD condition is violated in the case of Van der waals fluids. To illustrate this, we choose $\alpha = 0$ in (3.1). Hence, there is no dispersion and the limit as $\epsilon \to 0$ are expected to be classical shocks. We consider this *zero dispersion*

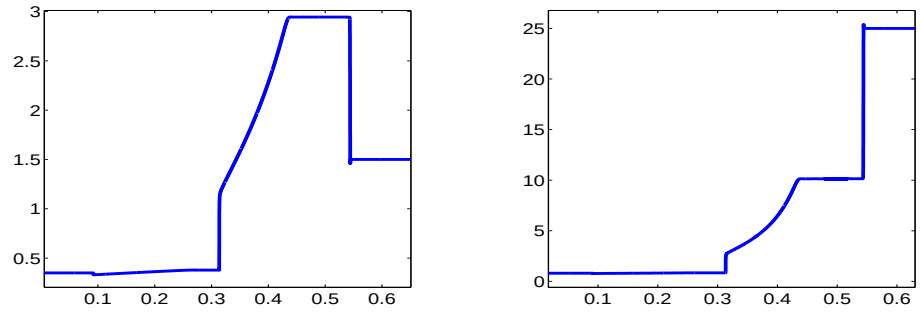

FIG. 3.3. *Approximation of the Riemann problem with initial data (3.9) resulting in large jump in volume τ. Left: Velocity u. Right: Volume τ, Results obtained with an eighth order WCD scheme with 25000 points.*

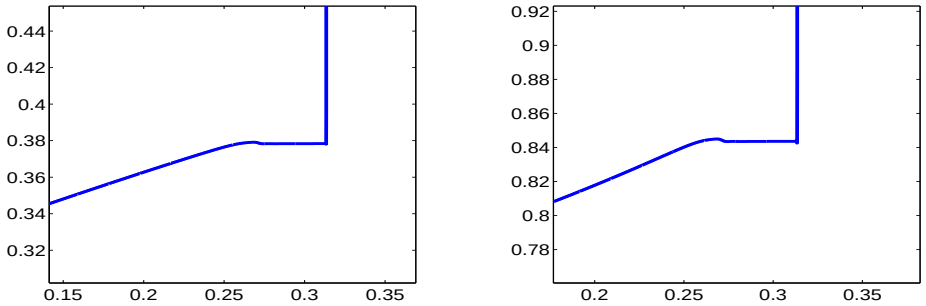

FIG. 3.4. *Zoom at nonclassical states in the approximation of the Riemann problem with initial data (3.9) resulting in large jump in volume τ. Left: Velocity u. Right: Volume τ, Results obtained with an eighth order WCD scheme with 25000 points.*

case and approximate the Riemann data (3.8) with a eighth-order WCD scheme with the coefficient $c = c_{WCD}$. The results of a mesh convergence study are shown in Figure 3.5. The results clearly show that the WCD scheme converges to the (correct) solution that contains a classical shock and a classical compound shock (shock followed by a rarefaction).

Next, we choose the coefficient $c = 0.1c_{WCD}$ in the eighth-order finite difference scheme (3.4). The solution is presented in Figure 3.6. The results clearly show that the approximate solution in fact converges to an incorrect solution that includes a *spurious* nonclassical shock instead of a rarefaction. This is indeed a surprising discovery that the failure to satisfy the WCD condition can result in the generation of spurious nonclassical shocks. This should be contrasted with those situations that where the correct nonclassical shocks may not be resolved by the finite difference scheme if the WCD condition is violated. As seen from Figure 3.6, once the coefficient c is increased to a sufficiently large value, the spurious nonclassical state is indeed removed and replaced by the correct rarefaction. In fact, a coefficient $c = 0.3c_{WCD}$ is enough to approximate the correct state and remove the nonclassical shock. This indicates that the WCD condition may not be sharp is all cases and is merely sufficient at approximating the correct solution. Furthermore, this example clearly suggests (from the equivalent equation) that the spurious nonclassical shock was generated due to the

contribution of higher-order dispersive terms in the equivalent equation, even when the underlying physical dispersion is switched off.

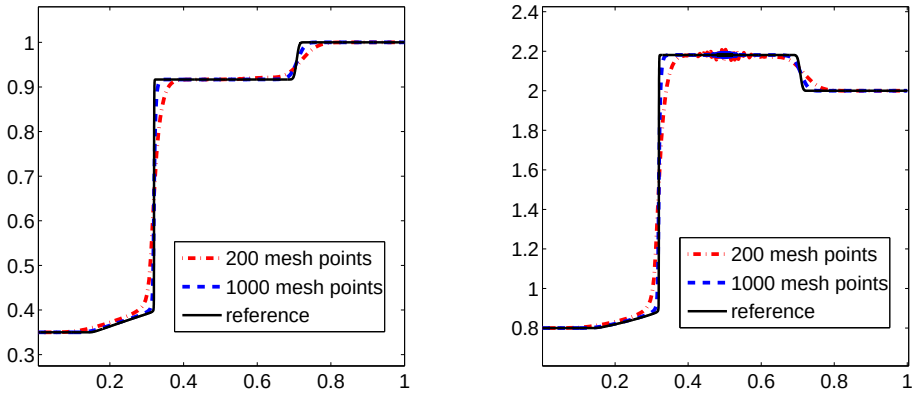

FIG. 3.5. *Convergence for the WCD scheme for the zero-dispersion limit of van der Waals fluid. Left: Velocity u. Right: Volume τ.*

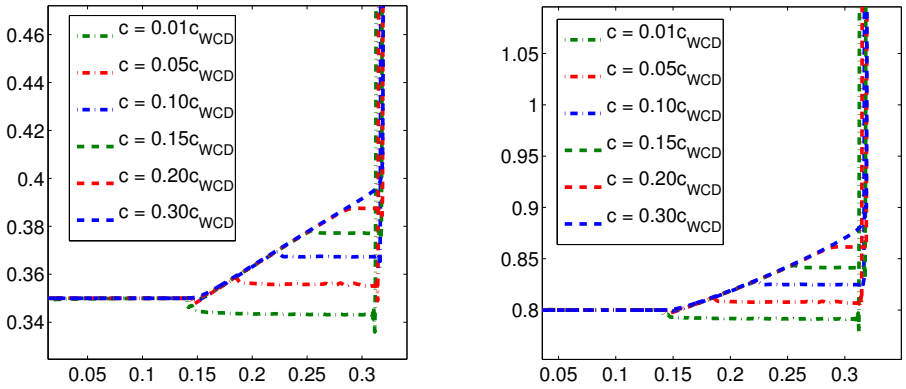

FIG. 3.6. *Spruious nonclassical states are observed for small values of the parameter c not satisfying the WCD condition (3.7) for the Van der waals fluid with zero dispersion. Left: Velocity u. Right: Volume τ*

4. WCD schemes for systems: a model of magnetohydrodynamics.

4.1. Fluids with viscosity and Hall effect. Many interesting systems of conservation laws in physics take the form

$$\mathbf{U}_t + \mathbf{F}_x = \epsilon D^{(1)}\mathbf{U}_{xx} + \alpha\epsilon D^{(2)}\mathbf{U}_{xx}. \tag{4.1}$$

Here, $\mathbf{U}, \mathbf{F}$ are the vector of unknowns and the flux vector, respectively and D^1, D^2 are matrices which model the viscosity and the Hall effect (dispersion). Observe that in contrast with scalar conservation laws, dispersion in systems of conservation laws can be modeled just in terms of second-order derivatives.

A prototypical (as well as motivating example) for such system of conservation laws (4.1) is provided by the model MHD equations with magnetic resistivity and Hall effect (see [30] and references therein),

$$
\begin{aligned}
v_t + ((v^2+w^2)v)_x &= \epsilon v_{xx} + \alpha\epsilon w_{xx}, \\
w_t + ((v^2+w^2)w)_x &= \epsilon w_{xx} - \alpha\epsilon v_{xx}.
\end{aligned} \tag{4.2}
$$

Clearly, the Hall MHD equations (4.2) can be recast in the general form (4.1) with $\mathbf{U} = \{v, w\}$ and

$$
D^{(1)} = \begin{pmatrix} 1 & 0 \\ 0 & 1 \end{pmatrix}, \qquad D^{(2)} = \begin{pmatrix} 0 & 1 \\ -1 & 0 \end{pmatrix}
$$

and $\mathbf{F} : R^2 \to R^2$ denotes the flux $\mathbf{F}(v,w) = \begin{pmatrix} (v^2+w^2)v \\ (v^2+w^2)w \end{pmatrix}$.

4.2. A class of WCD schemes. For any integer $p \geq 1$ we approximate (4.1) with the $2p$-th order consistent finite difference scheme

$$
\frac{d\mathbf{U}_i}{dt} + \frac{1}{\Delta x}\sum_{j=-p}^{j=p} \alpha_j \mathbf{F}_{i+j} = \frac{c}{\Delta x}\sum_{j=-p}^{j=p} \beta_j D^{(1)}\mathbf{U}_{i+j} + \frac{\alpha c}{\Delta x}\sum_{j=-p}^{j=p} \beta_j D^{(2)}\mathbf{U}_{i+j}. \tag{4.3}
$$

where $\mathbf{U}_i = \mathbf{U}(x_i, t)$, $\mathbf{F}_i = \mathbf{F}(\mathbf{U}_i)$ and the coefficients α_j and β_j need to satisfy the order conditions (2.4)-(2.5).

The equivalent equation of the finite difference scheme (4.3) is given by

$$
\begin{aligned}
\frac{d\mathbf{U}}{dt} = &\underbrace{-\mathbf{F}_x + c\Delta x D^{(1)}\mathbf{U}_{xx} + \alpha c \Delta x^2 D^{(2)}\mathbf{U}_{xx}}_{l.o.t} \\
&\underbrace{- \sum_{k=2p+1}^{\infty} \frac{\Delta x^{k-1}}{k!} A_k^p \mathbf{F}^{[k]} + c\sum_{k=2p+1}^{\infty} \frac{\Delta x^{k-1}}{k!} B_k^p D^{(1)}\mathbf{U}^{[k]} + \alpha c \sum_{k=2p+1}^{\infty} \frac{\Delta x^{k-1}}{k!} B_k^p D^{(2)}\mathbf{U}^{[k]}}_{h.o.t}
\end{aligned} \tag{4.4}
$$

The coefficients A_k^p and B_k^p are defined as in (2.8).

As for the scalar case and for the case of systems with viscosity and capillarity, we will analyze what happens at a single shock to derive the appropriate WCD condition in this particular case. The analysis is analogous to the previous example of a system with linear viscosity and capillarity. Assume that there exists a tolerance parameter τ such that $|h.o.t.| \leq \tau\,|l.o.t.|$ holds componentwise. Performing a similar analysis as for the previous example, we can impose an upper bound for the high-order terms given by the componentwise condition

$$
|h.o.t| \leq \left(\hat{S}_p^D c_i |\left\langle D_i^{(1)}, [\![\mathbf{U}]\!] \right\rangle| + \hat{S}_p^D |\alpha| c_i |\left\langle D_i^{(2)}, [\![\mathbf{U}]\!] \right\rangle| + \hat{S}_p^f \sigma |[\![\mathbf{U}_i]\!]|\right) \qquad (i = 1, 2)
$$

where $\hat{S}_p^D, \hat{S}_p^C, \hat{S}_p^f$ are defined as in (2.11) and σ is defined in (3.6). Furthermore, a lower bound for the low-order terms is given by

$$
|l.o.t| \geq \left(|\alpha| c_i |\left\langle D_i^{(2)}, [\![\mathbf{U}]\!] \right\rangle| + c_i |\left\langle D_i^{(1)}, [\![\mathbf{U}]\!] \right\rangle| - \sigma |[\![\mathbf{U}_i]\!]|\right) \qquad (i = 1, 2).
$$

Combining the two bounds we may obtain the condition $|h.o.t.| \leq \tau\,|l.o.t.|$ by ensuring the two simple linear conditions:

$$(4.5)\quad (\mathbf{WCD})_i: \quad \left(\left(|\alpha| - \frac{\hat{S}_p^D|\alpha|}{\tau}\right)|\left\langle D_i^{(2)}, [\![\mathbf{U}]\!]\right\rangle| + \left(1 - \frac{\hat{S}_p^D}{\tau}\right)|\left\langle D_i^{(1)}, [\![\mathbf{U}]\!]\right\rangle|\right) c_i - \left(1 + \frac{\hat{S}_p^f}{\tau}\right)\sigma|[\![\mathbf{U}_i]\!]| > 0$$

simultaneously. Observe that if $\left\langle D_i^{(1)}, [\![\mathbf{U}]\!]\right\rangle = 0$, we set the corresponding $c_i = 0$ for $i = 1, 2$. The scheme parameter c in (4.3) is defined as $c = \max_{i=1,2} c_i$.

4.3. Numerical experiments. We set $v = r\cos(\theta)$ and $w = r\sin(\theta)$ and consider initial Riemann problems of the form,

$$(4.6)\quad r(x,0) = \begin{cases} r_L, & x < 0.25, \\ 0.6r_L, & x > 0.25, \end{cases} \qquad \theta(x,0) = \begin{cases} \frac{3}{10}\pi, & x < 0.25, \\ \frac{13}{10}\pi, & x > 0.25. \end{cases}$$

The values of r_L and α will be varied in the subsequent experiments.

We consider the approximation of strong shocks by setting $r_L = 100$ and $r_L = 500$. The approximations, performed with an fourth-order WCD scheme on a mesh of 4000 uniformly spaced points is shown in Figure 4.1. The results clearly show that the solution consists of very large amplitude $\mathcal{O}(10^3)$ nonclassical shocks in both the unknowns. The fourth-order WCD scheme is able to approximate these very large nonclassical shocks quite well.

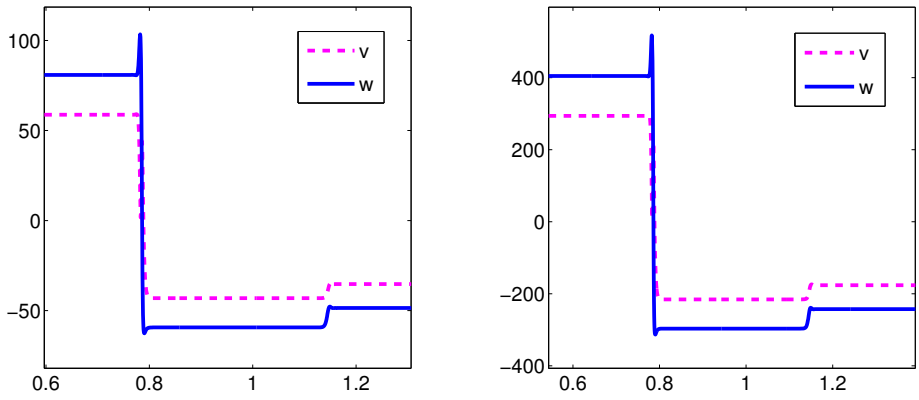

FIG. 4.1. *Large shocks in v and w-variable for the Hall MHD system (4.2 using a fourth order WCD scheme with* 4000 *mesh points.*

In order to characterize the nonclassical shocks for a large class of initial data, we compute the intermediate (nonclassical) state v_M with varying left state v_L. The results (for different values of the Hall coefficient α) are shown in Figure 4.2. Similar results for the intermediate state w_M with respect to varying left state w_L is shown in Figure 4.3. They clearly show that the WCD scheme is able to approximate nonclassical shocks of varying strengths (ranging from small to very large) efficiently. This should be contrasted with the results in [30] where only shocks of moderate strength could be computed.

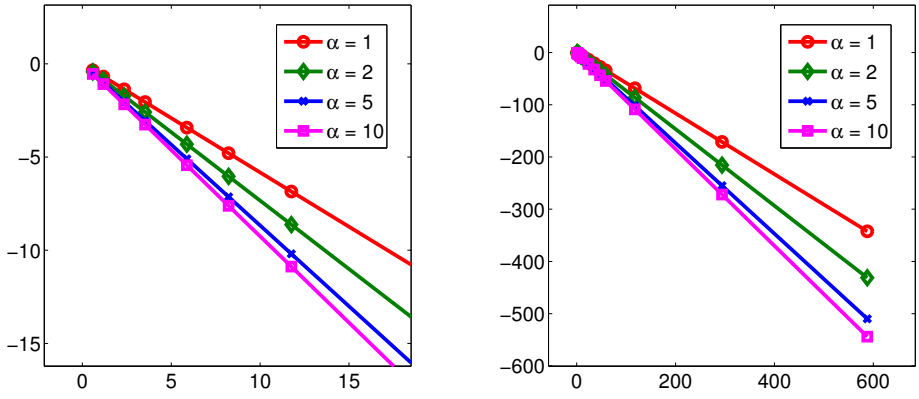

FIG. 4.2. *Intermediate state v_M (Y-axis) vs. left state v_L (X-axis) plot for the Hall MHD model (4.2, computed with a fourth-order WCD scheme.*

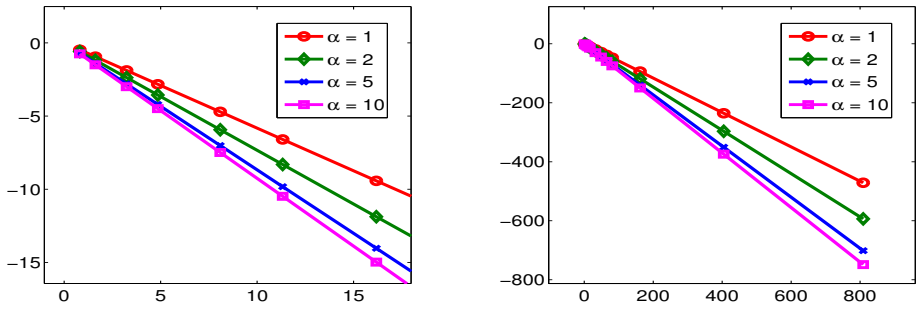

FIG. 4.3. *Intermediate state w_M (Y-axis) vs. left state w_L (X-axis) plot for the Hall MHD model (4.2, computed with a fourth-order WCD scheme.*

4.4. Computing the kinetic relation. We now examine the kinetic relations given in [30]

$$\phi(s) = -s\frac{1}{2}[\![v^2 + w^2]\!] + \frac{3}{4}[\![(v^2 + w^2)^2]\!]$$

numerically for $\alpha = 1, 2, 10$ using the 4-th order WCD scheme with $\tau = 0.1$ on a grid with $N = 4000$ mesh points. The numerical kinetic relations (scaled entropy dissipation vs. shock speed) are shown in Figure 4.4 and clearly indicate that the kinetic relation for the reduced MHD with Hall effect is given by

$$\phi(s) = k_\alpha s^2,$$

with a constant k_α that depends on the Hall coefficient α. Furthermore, the kinetic relation also demonstrate the ability of the WCD schemes to compute nonclassical shocks of arbitrary strength.

5. Concluding remarks. Systems of conservation laws are often derived by ignoring small-scale effects such as diffusion, resistivity, capillarity, and Hall effect.

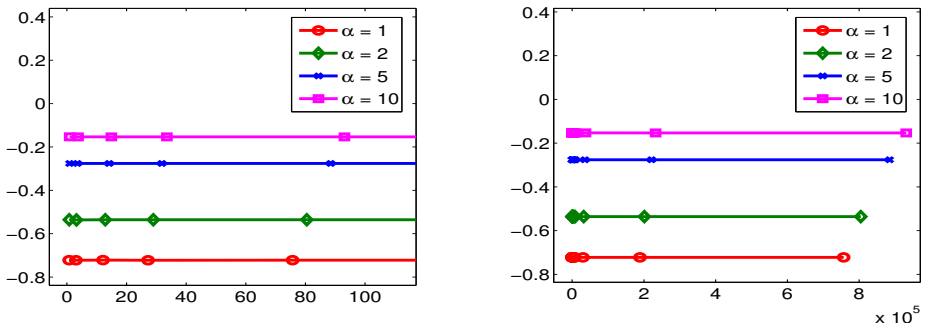

FIG. 4.4. *Scaled entropy dissipation* $\frac{\phi(s)}{s^2}$ *vs. shock speed* s *for the Hall MHD model (4.2, computed with a fourth-order WCD scheme.*

However, for many physically interesting systems of conservation laws, the limiting solutions depend explicitly on underlying small-scale effects. Examples include nonclassical shock waves that arise in nonconvex hyperbolic systems, nonconservative hyperbolic systems, and the initial boundary value problems. In such problems, a single entropy inequality alone does not suffice in ensuring uniqueness of weak solutions, and additional admissibility criteria such as kinetic relations, families of paths, or admissible boundary sets are necessary in order to single out the physically relevant solutions.

Standard numerical schemes such as finite difference schemes and finite volume schemes fail to approximate small-scale dependent shock waves correctly. This failure can be explained in terms of the equivalent equation of the scheme, which suggests that the leading-order numerical diffusion and dispersion terms for standard schemes are very different from the underlying physical diffusion and dispersion. Consequently, the schemes fail to approximate the physically relevant shock waves.

In the sucessive works [20, 18, 33, 32, 30, 36, 16, 7], various classes of schemes with "controlled dissipation" were developed. These schemes were designed such as the leading diffusion and dispersion terms of the equivalent equation matched the underlying physical diffusion and dispersion. These schemes were quite successful in resolving correct small scale dependent shock waves. However, the quality of approximation deteriorated as the shock strength was increased. In particular, the schemes with controlled diffusion failed to approximate large amplitude small scale dependent shock waves.

In the paper, we have proposed a new family of finite difference schemes – termed as schemes with well-controlled dissipation (WCD) which are designed to be able to approximate small scale dependent shock waves of arbitrary strength. The key idea behind these schemes relied on a refined analysis of the equivalent equation. In particular, the role of higher-order terms in the equivalent equation (often neglected in standard schemes) was elucidated. WCD schemes are designed such that the numerical amplitude of higher-order terms of the equivalent equation are controlled in terms of the leading diffusion and dispersion terms (to a user specified tolerance). This balance is ensured by choosing a (time and space dependent) coefficient of numerical diffusion and dispersion that satisfies the so-called WCD condition. The analysis suggests that for arbitrarily small tolerance parameters, one can always choose a sufficiently high-order finite difference discretization such that the WCD condition is

satisfied.

WCD schemes were tested on a large number of numerical experiments involving three different equations:

- The cubic conservation law with vanishing viscosity and dispersion.
- The Euler model of compressible fluids for a Van der Waals equation of state and vanishing diffusion and capillarity.
- A simplified model of magnetohydrodynamics with magnetic resistivity and Hall effect included.

For all three models, the WCD schemes were shown to perform remarkably well and, in particular, were able to correctly approximate small-scale dependent shock waves of arbitrarily large amplitude, as was demonstrated by computing the kinetic relation. These examples suggest that WCD schemes are able to handle configurations that are orders of magnitude more challenging than existing schemes at the current state of the art.

WCD schemes will be extended in future work (see [3]) in the following directions:

- Approximating small-scale dependent shock waves in nonconservative hyperbolic systems and for the boundary value problem.
- Systems of conservation laws in several space dimensions that contain small scale dependent shock waves as solutions, such in the full multi-dimensional MHD equations with resistivity and Hall effect.

REFERENCES

[1] R. Abeyaratne and J.K. Knowles, Kinetic relations and the propagation of phase boundaries in solids, Arch. Rational Mech. Anal. 114 (1991), 119–154.

[2] B. Audebert and F. Coquel, Hybrid Godunov-Glimm method for a nonconservative hyperbolic system with kinetic relations, in: Proc. on "Numerical mathematics and advanced applications", Springer Verlag, Berlin, 2006, pp. 646–653.

[3] A. Beljadid, P.G. LeFloch, and S. Mishra, Schemes with well-controled dissipation (WCD). Nonconservative systems and boundary layers, in preparation.

[4] C. Berthon and F. Coquel, Multiple solutions for compressible turbulent flow models, Commun. Math. Sci. 4 (2006), 497–511.

[5] C. Berthon, F. Coquel, and P.G. LeFloch, Why many theories of shock waves are necessary. Kinetic relations for nonconservative systems, Proc. Royal Soc. Edinburgh 137 (2012), 1–37.

[6] M.J. Castro, P.G. LeFloch, M.L. Munoz-Ruiz, and C. Pares, Why many theories of shock waves are necessary. Convergence error in formally path-consistent schemes, J. Comput. Phys. 227 (2008), 8107–8129.

[7] M.J. Castro, U.S. Fjordholm, S. Mishra, and C. Pares, Entropy conservative and entropy stable schemes for nonconservative hyperbolic systems, SIAM J. Num. Anal. (2013).

[8] C. Chalons, Transport-equilibrium schemes for computing nonclassical shocks. Scalar conservation laws, Numer. Methods Partial Differential Equations 24 (2008), 1127–1147.

[9] C. Chalons and P.G. LeFloch, High-order entropy conservative schemes and kinetic relations for van der Waals fluids, J. Comput. Phys. 167 (2001), 1–23.

[10] C. Chalons and P.G. LeFloch, A fully discrete scheme for diffusive-dispersive conservation laws, Numerische Math. 89 (2001), 493–509.

[11] C. Chalons and P.G. LeFloch, Computing undercompressive waves with the random choice scheme : nonclassical shock waves, Interfaces and Free Boundaries 5 (2003), 129–158.

[12] C.M. Dafermos, *Hyperbolic conservation laws in continuum physics,* Grundlehren Math. Wissenschaften Series 325, Springer Verlag, 2000.

[13] G. Dal Maso, P.G. LeFloch, and F. Murat, Definition and weak stability of nonconservative products, J. Math. Pures Appl. 74 (1995), 483–548.

[14] F. Dubois and P.G. LeFloch, Boundary conditions for nonlinear hyperbolic systems of conservation laws, J. Differential Equations 71 (1988), 93–122.

[15] R. Dutta, Personal communication to the authors, ETH Zürich, Switzerland, May 2013.

[16] U.S. Fjordholm and S. Mishra, Accurate numerical discretizations of nonconservative hyperbolic systems, M2AN Math. Model. Num. Anal. 46 (2012), 187–296.
[17] B.T. Hayes and P.G. LeFloch, Nonclassical shocks and kinetic relations. Scalar conservation laws, Arch. Rational Mech. Anal. 139 (1997), 1–56.
[18] B.T. Hayes and P.G. LeFloch, Nonclassical shocks and kinetic relations. Finite difference schemes, SIAM J. Numer. Anal. 35 (1998), 2169–2194.
[19] B.T. Hayes and P.G. LeFloch, Nonclassical shock waves and kinetic relations. Strictly hyperbolic systems, SIAM J. Math. Anal. 31 (2000), 941–991. (See also the internal report # 357, CMAP, Ecole Polytechnique, France, 1996.)
[20] T.Y. Hou and P.G. LeFloch, Why nonconservative schemes converge to wrong solutions. Error analysis, Math. of Comput. 62 (1994), 497–530.
[21] K.T. Joseph and P.G. LeFloch, Boundary layers in weak solutions to hyperbolic conservation laws, Arch. Rational Mech Anal. 147 (1999), 47–88. (See also the internal report # 341, CMAP, Ecole Polytechnique, France, 1996.)
[22] P.D. Lax, *Hyperbolic systems of conservation laws and the mathematical theory of shock waves,* Regional Confer. Series in Appl. Math. 11, SIAM, Philadelphia, 1973.
[23] P.G. LeFloch, Entropy weak solutions to nonlinear hyperbolic systems in nonconservative form, Comm. Part. Diff. Equa. 13 (1988), 669–727.
[24] P.G. LeFloch, Shock waves for nonlinear hyperbolic systems in nonconservative form, Institute for Math. and its Appl., Minneapolis, Publication # 593, 1989.
[25] P.G. LeFloch, Propagating phase boundaries: formulation of the problem and existence via the Glimm scheme, Arch. Rational Mech. Anal. 123 (1993), 153–197.
[26] P.G. LeFloch, An introduction to nonclassical shocks of systems of conservation laws, Lect. Notes Comput. Eng., Vol. 5, Springer Verlag, 1999, pp. 28–72.
[27] P.G. LeFloch, *Hyperbolic systems of conservation laws: the theory of classical and nonclassical shock waves,* Lecture Notes in Mathematics, ETH Zürich, Birkhäuser, 2002.
[28] P.G. LeFloch, Kinetic relations for undercompressive shock waves. Physical, mathematical, and numerical issues, Contemporary Mathematics, vol. 526, Amer. Math. Soc., Providence, RI, 2010, pp. 237–272.
[29] P.G. LeFloch, J.-M. Mercier, and C. Rohde, Fully discrete entropy conservative schemes of arbitrary order, SIAM J. Numer. Anal. 40 (2002), 1968–1992.
[30] P.G. LeFloch and S. Mishra, Nonclassical shocks and numerical kinetic relations for a model MHD system, Act. Math. Sci. 29 (2009), 1684–1702.
[31] P.G. LeFloch and S. Mishra, in preparation.
[32] P.G. LeFloch and M. Mohamadian, Why many shock wave theories are necessary. Fourth-order models, kinetic functions, and equivalent equations, J. Comput. Phys. 227 (2008), 4162–4189.
[33] P.G. LeFloch and C. Rohde, High-order schemes, entropy inequalities, and nonclassical shocks, SIAM J. Numer. Anal. 37 (2000), 2023–2060.
[34] R.J. LeVeque, *Finite volume methods for hyperbolic problems,* Cambridge University Press, 2003.
[35] C. Merkle and C. Rohde, The sharp-interface approach for fluids with phase change: Riemann problems and ghost fluid techniques, M2AN Math. Model. Numer. Anal. 41 (2007), 1089–1123.
[36] S. Mishra and L.V. Spinolo, Accurate numerical schemes for approximating intitial-boundary value problems for systems of conservation laws, Preprint 2011, SAM report 2011-57, ETH Zürich.
[37] M. Slemrod, Admissibility criteria for propagating phase boundaries in a van der Waals fluid, Arch. Rational Mech. Anal. 81 (1983), 301–315.
[38] E. Tadmor, The numerical viscosity of entropy stable schemes for systems of conservation laws. I, Math. Comp. 49 (1987), 91–103.
[39] E. Tadmor, Entropy stability theory for difference approximations of nonlinear conservation laws and related time-dependent problems, Acta Numer. 12 (2003), 451–512.
[40] E. Tadmor and W. Zhong, Entropy stable approximations of Navier-Stokes equations with no artificial numerical viscosity, J. Hyperbolic Differ. Equ. 3 (2006), 529–559.
[41] L. Truskinovsky, Dynamics of non-equilibrium phase boundaries in a heat conducting non-linear elastic medium, J. Appl. Math. Mech. (PMM), 51 (1987), 777–784.
[42] A.I. Volpert, The space BV and quasi-linear equations, Mat. USSR Sb. 2 (1967), 225–267.

Recent Research Reports

Nr.	Authors/Title

2013-31 R. Hiptmair and A. Moiola and I. Perugia
Plane Wave Discontinuous Galerkin Methods: Exponential Convergence of the hp-version

2013-32 U. Koley and N. Risebro and Ch. Schwab and F. Weber
Multilevel Monte Carlo for random degenerate scalar convection diffusion equation

2013-33 A. Barth and Ch. Schwab and J. Sukys
Multilevel Monte Carlo approximations of statistical solutions to the Navier-Stokes equation

2013-34 M. Hutzenthaler and A. Jentzen and X. Wang
Exponential integrability properties of numerical approximation processes for nonlinear stochastic differential equations

2013-35 S. Cox and M. Hutzenthaler and A. Jentzen
Local Lipschitz continuity in the initial value and strong completeness for nonlinear stochastic differential equations

2013-36 S. Becker and A. Jentzen and P. Kloeden
An exponential Wagner-Platen type scheme for SPDEs

2013-37 D. Bloemker and A. Jentzen
Galerkin approximations for the stochastic Burgers equation

2013-38 W. E and A. Jentzen and H. Shen
Renormalized powers of Ornstein-Uhlenbeck processes and well-posedness of stochastic Ginzburg-Landau equations

2013-39 D. Schoetzau and Ch. Schwab and T.P. Wihler
hp-dGFEM for Second-Order Mixed Elliptic Problems in Polyhedra

2013-40 S. Mishra and F. Fuchs and A. McMurry and N.H. Risebro
EXPLICIT AND IMPLICIT FINITE VOLUME SCHEMES FOR